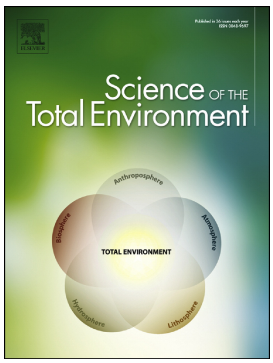

Organic matter preservation through complexation with iron minerals in two basins of a dimictic boreal lake with contrasting deep water redox regimes

Azadeh Joshani, Yeganeh Mirzaei, Andrew Barber, Kathryn Balind, Charles Gobeil, Yves Gélinas

PII: S0048-9697(24)01919-3

DOI: https://doi.org/10.1016/j.scitotenv.2024.171776

Reference: STOTEN 171776

To appear in: *Science of the Total Environment*

Received date: 3 November 2023

Revised date: 6 March 2024

Accepted date: 15 March 2024

Please cite this article as: A. Joshani, Y. Mirzaei, A. Barber, et al., Organic matter preservation through complexation with iron minerals in two basins of a dimictic boreal lake with contrasting deep water redox regimes, *Science of the Total Environment* (2023), https://doi.org/10.1016/j.scitotenv.2024.171776

Organic matter preservation through complexation with iron minerals in two basins of a dimictic boreal lake with contrasting deep water redox regimes

Azadeh Joshani[1], Yeganeh Mirzaei[1], Andrew Barber[1], Kathryn Balind[1], Charles Gobeil[2], and Yves Gélinas[1*]

[1] GEOTOP and Department of Chemistry and Biochemistry, Concordia University, 7141 Sherbrooke West, Montreal, QC, Canada, H4B 1R6

[2] INRS-Eau Terre Environnement, 490 rue de la Couronne, Université du Québec, QC, Canada, G1K 9A9

* Corresponding author:

Yves Gélinas
Department of Chemistry and Biochemistry
Concordia University
7141 Sherbrooke Street West
Montréal, QC, Canada, H4B-1R6
Tel.: 514-848-2424, ext. 3337
Email: yves.gelinas@concordia.ca
ORCID: 0000-0001-5751-8378

List of keywords: Lake sediment, iron, organic carbon preservation, stable carbon and nitrogen isotopes, FTIR

Key points:

- Iron plays an important role in the preservation of lacustrine sedimentary organic matter
- Chemical composition rather than redox conditions control the association between iron and organic matter
- OC:Fe ratios should not be used to infer a formation mechanism between iron and organic carbon

Abstract

The biogeochemical cycles of iron and organic carbon (OC) are closely interconnected in terrestrial and aquatic systems. In ocean waters, the concentration of reactive Fe is tightly controlled by soluble organic ligands. In soils, Fe stabilizes OC by forming aggregates that shield OC from degradation. In lake sediments however, the role of Fe in the preservation of OC has not been explored as extensively yet. We investigated Fe-OC interactions in sediment collected from Lake Tantaré, in which two basins are characterized by contrasting redox conditions. These contrasting redox conditions provide an opportunity to assess their importance in the formation of stable Fe-OC complexes. On average, 30.1 ± 6.4 % of total OC was liberated upon reductively dissolving reactive iron. The Fe-associated and the non-Fe-associated OC pools were characterized at the elemental (OC, TN), isotopic ($\delta^{13}C$, $\delta^{15}N$) and functional group (FTIR) levels. Large differences in OC:Fe and TN:Fe ratios between the two basins were found which were not linked to OM chemical composition but rather to differences in reactive iron concentrations stemming from the higher abundance of iron sulfides in the anoxic basin. Nevertheless, since the affinity of OM for iron sulfides is lower than that for iron hydroxides, using OC:Fe and TN:Fe ratios as a diagnostic tool for the type of OM-Fe interactions should be done with care in anoxic environment. Same caution should be considered for oxic sediments due to the variation of the proportion of iron hydroxides associated with OM from sample to sample.

Introduction

Human activities have significantly affected the global carbon cycle over the past 200 years, leading to a concentration of carbon dioxide (CO_2) in the atmosphere to be about 50% higher now than early period of Industrial Revolution (Vitousek et al., 1997; Falkowski et al., 2000). The major natural removal pathway for atmospheric CO_2 is photosynthesis of organic matter (OM) on land and the surface ocean. Most newly synthesized OM is rapidly oxidized back to inorganic carbon and other nutrients, and eventually returns to the atmosphere as CO_2. In the ocean, less than 1% of the yearly oceanic primary production of organic carbon (OC) is ultimately buried and preserved in sediments (Galy et al., 2007). Sedimentary burial and preservation of OC upholds the delicate balance of O_2 and CO_2 in the atmosphere on geological time scales by maintaining the balance between primary production and respiration (Hartnett et al., 1998; Burdige et al., 2007). OM burial also represents a long-term sink for redox-sensitive elements (such as C, N, S, Mn, and Fe) in global biogeochemical cycles (Thamdrup et al., 1994; Hedges et al., 1995; Straub et al., 1996; Lalonde et al., 2012).

Several factors play a role in long-term OC burial efficiency, such as OC degradation rate (Canfield et al., 1994), primary productivity (Hedges et al., 1995), sedimentation rate (Müller and Suess, 1979; Henrichs et al., 1987) and low bottom water oxygen concentration (Demaison et al., 1980; Betts and Holland, 1991; Paropkari et al, 1992; Hartnett and Devol, 2003), but the exact controls on OM preservation still remain unclear (Hedges et al., 1995; Burdige et al., 2007). The close interactions

between organic and inorganic sedimentary materials have long been recognized as one of the most important preservation mechanisms by which OC is physically protected through shielding or encapsulation, leading to steric hindrance (Ingalls et al., 2003; Arnason and Keil, 2007). Physical protection as a preservation mechanism is supported by the observation that more than 90% of preserved OC is very closely associated with minerals in most marine sediments (Keil et al., 1994; Kennedy et al., 2011).

The interactions between organic and inorganic minerals have traditionally been considered uniquely as chemical or physical adsorption processes on the surface of minerals such as clays and iron hydroxides. Such thermodynamic equilibrium interactions are however reversible and cannot explain the long-term preservation of molecules that are labile when dissolved in sediment pore waters (Meyer, 1995). Lalonde et al. (2012) and Barber et al. (2017) proposed a mechanism of physical protection involving the formation of inner-sphere complexes between organic compounds and nanophase iron hydroxide particles. They estimated that an average of 21.5 ± 8.6% of the total OC in marine sediments, representing highly contrasting depositional settings, is directly attached to reducible, or reactive, solid iron phases (Lalonde et al., 2012). Extrapolating to the global ocean, this estimation corresponds to a total mass of OC directly associated to reactive iron of 19–45 × 10^{15} g (Lalonde et al., 2012). Interestingly, 26.4% of total OC was directly associated to Fe in the surface sediment of Lake Brock, the only lake sediment studied by Lalonde et al. (2012), suggesting that OC-Fe interactions also play a role in OC preservation in freshwater systems.

The concentrations of iron and OC co-vary in sediments (Berner, 1970), but elucidating the exact nature of the chemical bonds between OC and iron under contrasting redox conditions is extremely challenging because of the complicated chemistry of iron and OC near the sediment-water interface (SWI) and oxic-anoxic redox boundaries within the sediment. In addition to chemi- and physisorption, sedimentary OM can interact with iron hydroxides through a ligand-exchange mechanism where electronegative functional groups such as carboxyl, phenol or alcohol replace the hydroxyl groups of iron hydroxide particles (Gu et al., 1994; Kaiser et al., 1997). At the SWI, where oxygen from the water column diffuses through the uppermost layers of the sediment, Fe(III) is thermodynamically stable mostly as solid phase (Fe hydroxides), but also other less easily reducible iron containing minerals such as clays (Viollier et al., 2000). Below the oxic/anoxic interface Fe(III) can be reductively dissolved to soluble Fe(II) (Voillier et al., 2000) that can sorb onto solid particles or diffuse either upwards towards the oxic zone where it is re-oxidized, or downward and precipitate as iron sulfides. The re-oxidation of Fe(II) above the redox transition zone leads to the formation of iron hydroxide nanoparticles that interact strongly with OC owing to their chemical composition and high surface areas. While pH and competing anions (sulfate and phosphate in particular) dictate the adsorption of OM onto different types of iron oxides such as ferrihydrite, goethite and haematite (Gu et al., 1994), co-precipitation between OM and Fe nanoparticles would lead to the formation of surface-active Fe-OC complexes (or aggregates). Aggregation of this type is analogous to the onion model of Mackey and Zirino (1994). It would result in a decrease in the reduction rate of Fe(III)

under anoxic conditions, which would explain the persistence of reducible iron in anoxic sediments for thousands of years (Haese et al., 1997), and to a decrease in OM degradation rates leading to higher OM burial efficiencies (Boudot et al., 1989; Jones and Edwards, 1998).

Organic carbon burial and preservation in lentic ecosystems such as lakes, reservoirs, ponds and impoundments is poorly constrained because of the absence of comprehensive datasets, particularly for small water bodies. Several studies have shown that the OC burial rates in these systems should be taken into account in global carbon cycle analyses even if they cover a small fraction of the Earth's land surface area (Cole et al., 2001; Sobek et al., 2003; Pace et al., 2005; Clow et al., 2015; Ferland et al., 2012). The main objectives of this work are to understand the role of the Fe-OC interactions in the preservation of OC in lake sediments, and to assess the importance of redox conditions in the formation of stable Fe-OC aggregates. We used sediments collected from Lake Tantaré located in Quebec, Canada. The lake is a freshwater aquatic system with four basins, two of which, Basin A and Basin B, being characterized by seasonally contrasting bottom water redox conditions owing to contrasting sediment accumulation rates and water column depth. These differing redox conditions provide an opportunity to test our hypothesis regarding the importance of redox transitions in the formation of these stable OC-Fe complexes. The Fe-associated and the non-Fe-associated OC pools were characterized using elemental (organic carbon and total nitrogen) and isotopic ($\delta^{13}C$, $\delta^{15}N$) analysis, and their chemical composition was assessed by Fourier-transform infrared (FTIR) spectroscopy.

Materials and Methods

Study Site

Lake Tantaré (47°04'15''N, 71°33'42'' W, Figure 1) is a small (1.1 km^2) oligotrophic lake located in an ecological reserve 40 km northwest of Québec City, in the province of Québec. This dimictic soft water lake, sitting on a granite and gneiss bedrock of the Canadian Precambrian Shield, is characterized by low concentrations of dissolved organic carbon (DOC; 2.2–2.8 mg L^{-1}) (Liu et al., 2015). Since the lake basin is uninhabited, metal ions are only introduced to this lake through natural weathering and atmospheric deposition as the impact of human activities is negligible (Alfaro-De la Torre et al., 2000). Lake Tantaré is comprised of four basins that are separated by shallow sills. In this study, we used sediments from Basin A (pH of 5.5-5.8), which is has maximum depth of 15 m and perennially oxic conditions (> 3.8 mg O_2 L^{-1}), as well as from Basin B (pH of 6.6-7.0) which has a maximum depth of 21 m and is characterized by seasonal variations in redox conditions as bottom waters become anoxic (< 0.01 mg O_2 L^{-1}) during late summer-early fall (Figure 1) (Couture et al., 2008; 2009).

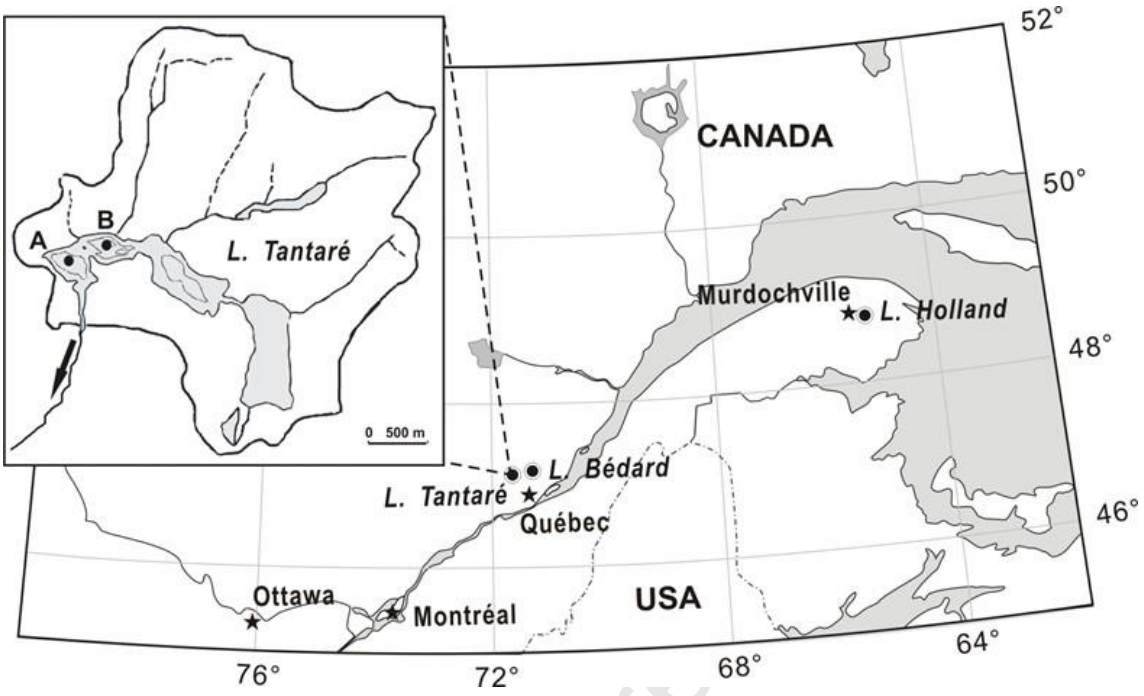

Figure 1. Map showing the location of Lake Tantaré.

Sampling and Sediment Dating

Sediment cores were collected in both basins in August 2013 using butyrate tubes with an inner diameter of 9.5 cm. Sediment were sliced at 0.5- or 1-cm intervals down to 25 cm. The sediment samples were freeze-dried and stored in clean polyethylene containers. Depth profiles were transformed into their corresponding age profiles to allow direct comparison of the data from Basins A and B. The age model was developed by Tessier and coworkers (Tessier et al., 2014).

Reduction Method

The reductive extraction used in this study was adapted from a method originally developed for quantifying reactive (reducible) iron in soils (Mehra and Jackson, 1960). It

was modified to allow measuring the concomitant removal of OC (by elemental analysis coupled to an isotope ratio mass spectrometer, or EA-IRMS) and iron (by inductively coupled plasma mass spectrometry, or ICP-MS) from the marine and lake sediments (Lalonde et al., 2012). In this method, sodium dithionite was used to reductively solubilize Fe(III) oxides to Fe(II), along with citrate, a water-soluble complexing agent that keeps reduced iron in the dissolved phase. The OC solubilized during the reduction step was measured by difference by elemental analysis (total mass of OC before reduction – total mass of OC after reduction = mass of OC solubilized). The reduction reaction was carried out under buffered conditions (bicarbonate) to maintain the pH at 7.0 ± 0.3. The OC released upon the reduction reaction is considered specifically associated with iron oxides as other reducible mineral phases such as manganese oxides are much less abundant in sediments (Feyte et al., 2010; 2012). In order to take into account desorbed OC from sediment at the temperature and ionic strength used for the reduction reaction, a preliminary control experiment was performed on the sediment prior to the reduction step by replacing the citrate and dithionate with sodium chloride, maintaining the same ionic strength as in reduction experiment (Lalonde et al., 2012).

EA-IRMS Measurements

The certified standard materials Sucrose (IAEA-CH-6; $\delta^{13}C$ = -10.45 ± 0.07 ‰), Polyethylene (IAEA-CH-7; $\delta^{13}C$ = -32.15 ± 0.10 ‰) and Ammonium Sulfate (USGS24; $\delta^{15}N$ = -30.41 ± 0.27‰;), as well as *ß*-alanine (Sigma-Aldrich; $\delta^{13}C$ = -26.18 ± 0.10 ‰; OC = 40.44%; $\delta^{15}N$ = -2.21 ± 0.24‰; %TN = 15.7%) and sucrose (Sigma-Aldrich; $\delta^{13}C$ = -11.77 ± 0.09 ‰; OC = 42.11%), two in-house standards calibrated with these certified reference

materials, were used for calibration purposes. The $\delta^{13}C$ and organic carbon concentration analyses were carried out using an EuroEA3000 CHNS-O analyzer (EuroVector S.p.A.) coupled to an Isoprime 100 IRMS (Elementar Americas Inc.). The stable carbon isotope ratios are expressed relative to the international reference standard Vienna Peedee Belemnite (VPDB). Precision and accuracy of the measured stable isotope values were assessed using a range of masses of the pure in-house calibrated compound (*ß*-alanine) and IAEA certified sucrose covering the entire dynamic range of the instrument. The %OC and $\delta^{13}C$ values were obtained before and after the removal of OM associated with iron oxide, and the value of Fe-associated OC was calculated using an isotopic mass balance model. In order to remove inorganic carbon (i.e., carbonates) prior to EA-IRMS measurement, the freeze-dried sediment samples were weighed into silver (Ag) capsules, exposed to 12 M HCl vapor for 12 hours, followed by a 1-hr heating step at 50°C and 6 hours in a desiccator to remove residual water/acid (Hedges and Stern, 1984). The Ag capsules containing the decarbonated samples were then sealed and wrapped in a tin capsule before EA-IRMS analysis.

FTIR and ICP-MS Measurements

FTIR analyses were carried out on the sediments before (initial) and after (residual) the removal of OM associated with iron hydroxides. Subsamples from depths of 1-2 cm, 8-9 cm and 19-20 cm were analyzed, corresponding to ages of 12.6, 96.0 and 232.8 years, respectively, for Basin A, and ages of 6.3, 43.3 and 132.2 years, respectively, for Basin B due to difference in their sediment accumulation rates. A mass of 3.0 ± 0.1 mg of each freeze-dried subsample was carefully homogenized with 100.0 ±

0.3 mg of dry potassium bromide using a mortar and pestle. All of the homogenized mass was used to make a compressed pellet. Prior to acquiring the spectrum, the pellet chamber was purged with nitrogen for a minimum of 5 min to remove water vapor and the carbon dioxide signal at 2350 cm^{-1}. The measurements were done on a Nicolet 6700 FTIR spectrophotometer (128 scans at a resolution of 2 cm^{-1}). An Agilent 7500 ICP-MS was used to measure iron concentrations by external calibration following appropriate dilution of the samples.

Results and discussion

Elemental and Isotopic Composition

The vertical distribution of reducible Fe, OC, and total N, as well as the OC:Fe and C:N atomic ratios, and the stable isotope values of carbon ($\delta^{13}C$) and nitrogen ($\delta^{15}N$) were determined in sediment cores of the perennially oxygenated Basin A and the seasonally anoxic Basin B of Lake Tantaré (Figures 2 and 3, and Table S1).

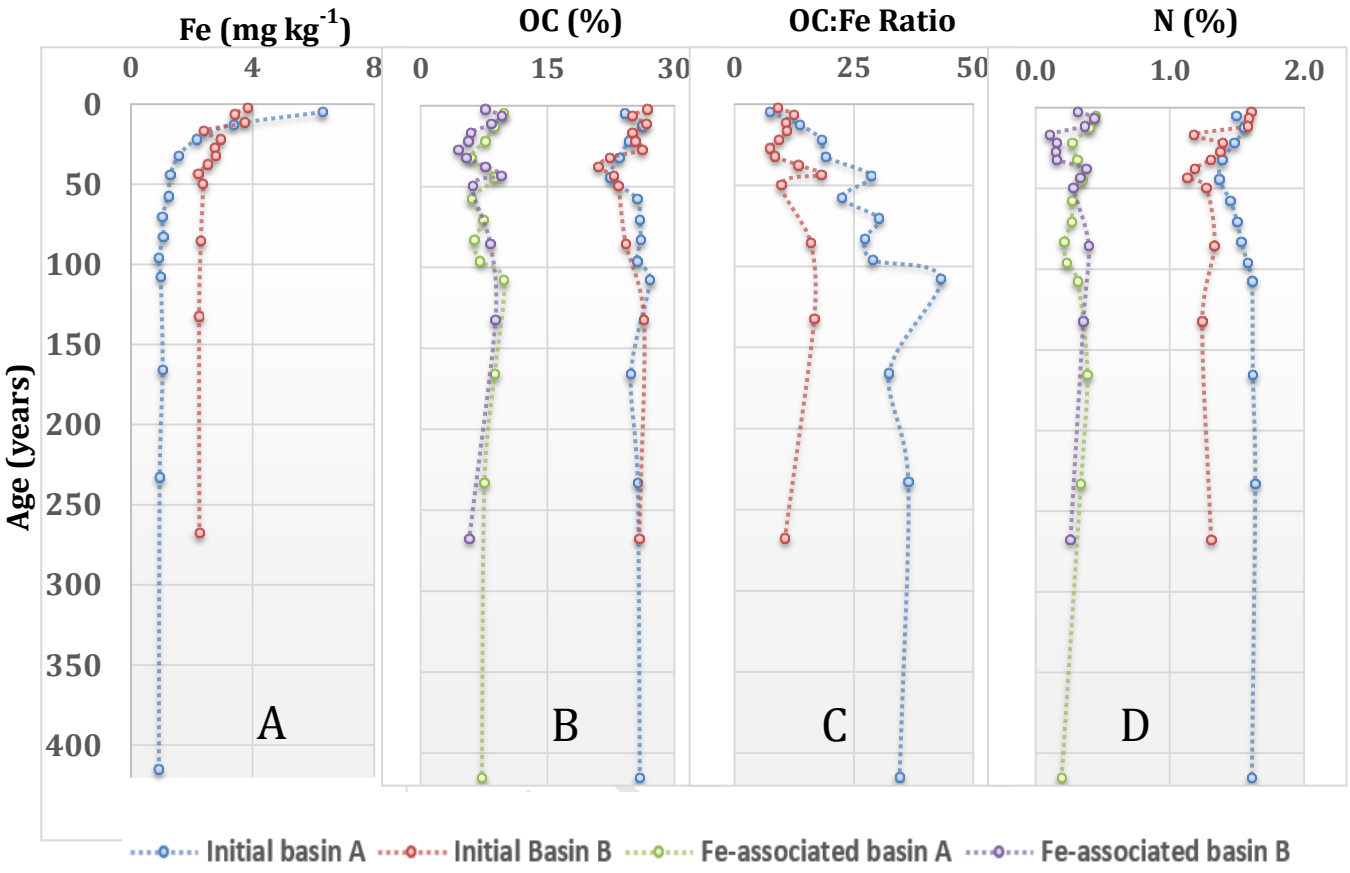

Figure 2. Age profiles of (A) the concentration of reducible Fe; and (B) organic carbon (OC); (C) the OC:Fe molar ratios; and (D) the concentration of nitrogen (N) before (Initial) and after extraction (Fe associated) in Basins A and B. Each point represents the average value of triplicate measurements. Standard deviation bars were omitted for clarity but values can be found in Table S1 (Supporting Information).

Reducible Fe concentrations were high below the SWI in Basin A (6.3% of the total mass) and decreased sharply to about 1% at 2-3 cm of depth (corresponding to an age of ~22 yrs) to reach nearly constant concentrations deeper in the sediment (Figure 2A). The enrichment of Fe(III) hydroxides below the SWI matches with the results of previous studies conducted on the same basin (Fortin et al., 1993; Heiri et al.; 2001;

Chappaz et al., 2008; Couture et al., 2009) and is due to the recycling of Fe at depth (partial dissolution of Fe(III) oxides, release of dissolved Fe(II) to pore waters, followed by its migration towards the near surface oxic layer where it is re-oxidized to Fe(III) hydroxides, and at depth where it can react with dissolved sulfides to form mackinawite or pyrite) (Laforte et al., 2005; Liu et al., 2015). As also observed by Couture et al. (2008) and Feyte et al. (2010), dissolved Fe(II) in the pore waters of Basin B is partly lost through diffusion to the water column owing to the absence of an oxic sediment layer near the SWI, hence explaining the absence of an enrichment in Fe(III) hydroxides in this core (Fe concentrations between 2.2 and 3.8% throughout). The downward diffusing Fe(II) reacting with sulfide may however explain the higher reactive iron concentrations in this core given the absence of a Fe(III) hydroxides sink near the SWI and the higher pH conditions in the bottom water of Basin B compared to Basin A (6.6-7.0 *vs.* 5.5-5.8, respectively (Feyte et al., 2010), as iron monosulfide solubility increases with decreasing pH (Wolthers et al., 2005). While Couture et al. (2009) reported that the concentration of acid volatile sulfides (AVS) was low and thus contributed little to reduced Fe solid phases in Basin A (Couture et al., 2009), AVS concentrations were about an order of magnitude higher in Basin B (Couture et al., 2017).

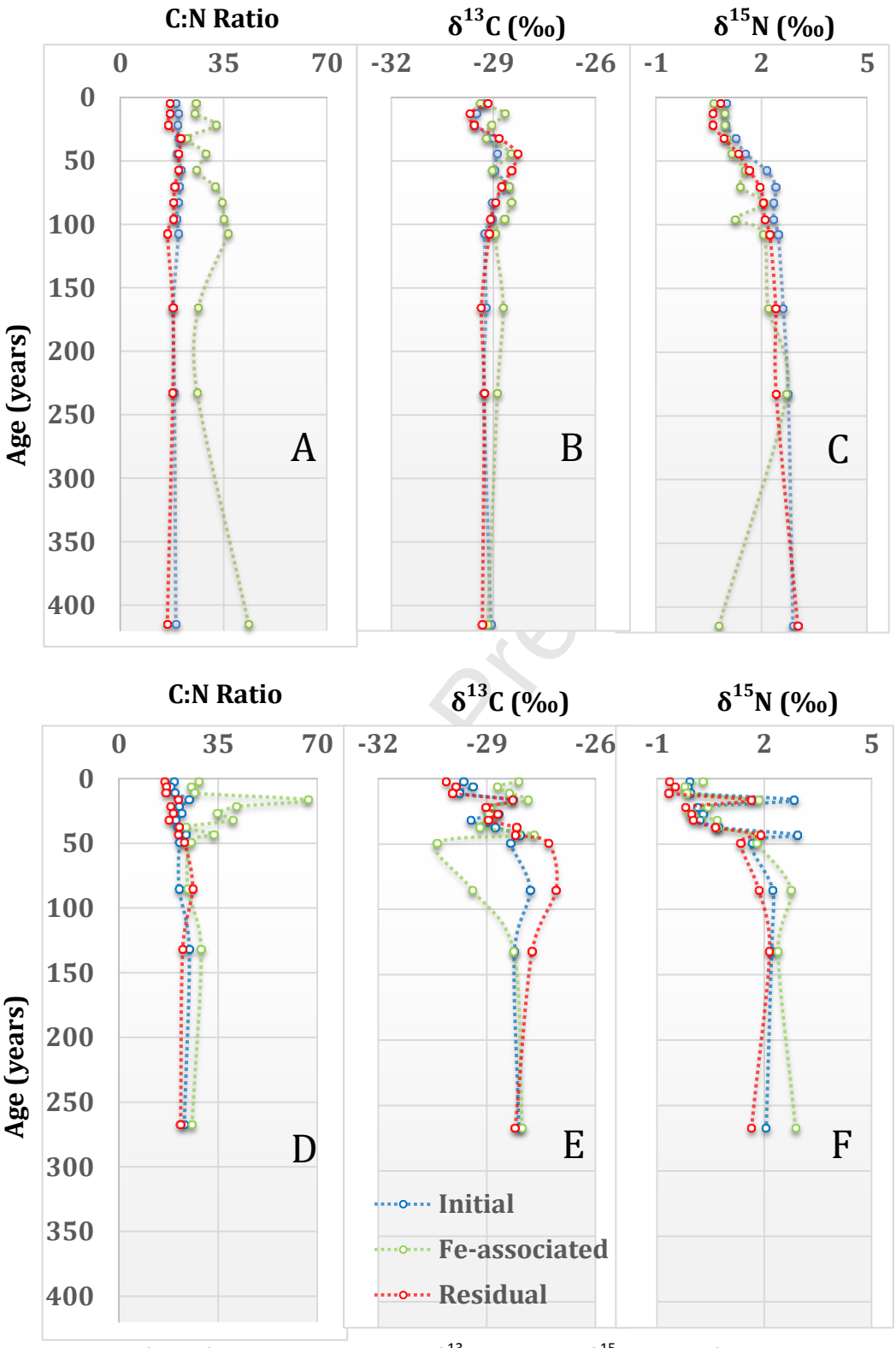

Figure 3. Age profiles of the C:N atomic ratio, $\delta^{13}C$ value and $\delta^{15}N$ value of initial and residual sediments in basin A (A, B, and C, respectively) and basin B (D, E, and F, respectively). Each point

represents the average value of triplicate measurements. Standard deviations bars were omitted for clarity but values can be found in Table S1 (Supporting Information).

The total OC concentrations were similar in both basins and ranged between 22.4 ± 0.7 % and 27.1 ± 0.3 % for Basin A, and 21.0 ± 0.5 % to 26.8 ± 0.3 % for Basin B (Figure 2B), with small, yet generally synchronous variations in the past century (Laforte et al., 2005). These values are in agreement with the data reported by Feyte et al. (2010). The concentrations of OC associated with iron (Fe-associated OC) averaged 7.5 ± 1.6% of the total sediment mass in the two basins (Figure 2B), corresponding to 30.1 ± 6.4% of total OC in Basins A and B. These values are similar to the results obtained for other lake sediments analyzed using this method, and are on the high end of the range of percentages measured for a series of marine sediments by Lalonde et al. (2012). Noteworthy, the highest total OC concentration in Lalonde's sediment sample set was 6.9 wt% compared to 20-28 wt% for Lake Tantaré, which suggests that the conclusions reached for marine sediment also apply to organic-rich lake sediments despite the lower relative proportion of inorganic matter in the latter.

High OC:Fe molar ratios were found in both basins, suggesting close interactions between OC and Fe in these samples. The ratios have remained similar in both basins near the SWI for the past ~20 years (Fig. 2C), but they diverge considerably deeper in the sediment with averages of 26.4 ± 0.6 and 11.8 ± 0.7 for Basin A and B, respectively (Figure 2C). The differences in the OC:Fe and TN:Fe (Supporting Information Table S1) profiles between the two adjacent basins exposed to similar OC and inorganic material inputs (although at a higher rate in Basin B), but dissimilar oxygen exposure regimes,

suggests two possible scenarios. First, the contrasting ratios could reflect differences in OM chemical composition driven by the different redox regimes in two basins (Coward et al., 2018), or they could be due to the presence of a pool of reactive iron with a generally lower affinity for OM in Basin B, thus leading to lower OC:Fe ratios.

Total nitrogen concentrations varied between 1.4 ± 0.4 % and 1.6 ± 0.4 % in Basin A, and 1.1 ± 0.5 % and 1.6 ± 0.4 % in Basin B (Figure 2D). Total N concentrations were slightly lower at depth in Basin B compared to Basin A, a difference not paralleled in the concentration of nitrogen associated to iron (Figure 2D). The concentrations of Fe-associated nitrogen varied between 0.15 and 0.50 % in both basins, corresponding to between 9 and 31% of total N. This range is also consistent with the finding of Lalonde et al. (2012) for boreal lake sediments (21-34 %), but is higher than in marine sediments, for which the highest measured percentage of Fe-associated nitrogen was 15.3 % (average of 6.0 ± 5.2 % for the entire dataset), suggesting that the coupling of iron and nitrogen is stronger in continental aquatic systems where OM is more depleted in nitrogen compared to marine OM.

The C:N atomic ratios for the initial and residual (e.g., non-Fe-associated OM) fractions of the sediments vary little with age and between basins, with averages of 19.3 ± 1.4 and 21.6 ± 1.1 in Basins A and B, respectively (Figure 3A and 3D). These ratios are higher than those measured for settling particles of productive lakes (6-9; Hamilton-Taylor et al., 1984) and are typical of soil OM, reflecting the predominance of allochthonous OM inputs in the sediments of Lake Tantaré (Bordovskiy, 1965; Thornton and McManus, 1994). The C:N ratios are higher for Fe-associated OM throughout the

core in Basin A, and for sediment deposited in the past 50 years in Basin B (Figure 2D, suggesting that the OM associated with Fe hydroxides is depleted in N relative to non Fe-associated OM. This observation agrees with the results from a long-term incubation experiment in which it was proposed that iron oxides lead to the preferential preservation of OC and, in parallel, to an enhancement in the removal of nitrogen-rich OM (Barber et al., 2014). Additional work is needed to confirm this hypothesis.

The $\delta^{13}C$ and $\delta^{15}N$ stable isotope values measured for total OM as well as for the Fe-associated and residual OM fractions were similar and varied little with time in Basin A, aside from a 1.0 to 1.5 ‰ lower $\delta^{15}N$ value for sediment deposited in the past ~75 years. This is not the case for Basin B where $\delta^{13}C$ values of the three fractions varied by more than 2.5 ‰, particularly near the surface and between 50 and 100 years ago. (Figure 3E). The reason for these differences is not fully understood but may have to do with biochemical fractionation upon Fe-OM co-precipitation.

Two sharp peaks centered around 15 and 45 years characterized the $\delta^{15}N$ profile for total OM and the Fe-associated and residual fractions, with an enrichment as large as 3.0 ‰ at these depths (Figure 3F), where the total N concentration was also the lowest (Figure 2D). This result likely is linked to N degradation pathways and agrees with the inverse relationship found between total N and $\delta^{15}N$ in sediments from temperate lakes (Botrel et al., 2014).

OM chemical composition

The FTIR spectra of the total, residual and Fe-associated OM are presented for the two basins in Figure 4. For each sample, the spectra for total OM and the control-treated samples (see Materials and Methods section) were virtually indistinguishable from one another therefore the former were used for the discussion below. The small fraction of OM lost during the control treatment was thus very similar in chemical composition to the insoluble OM remaining after the treatment.

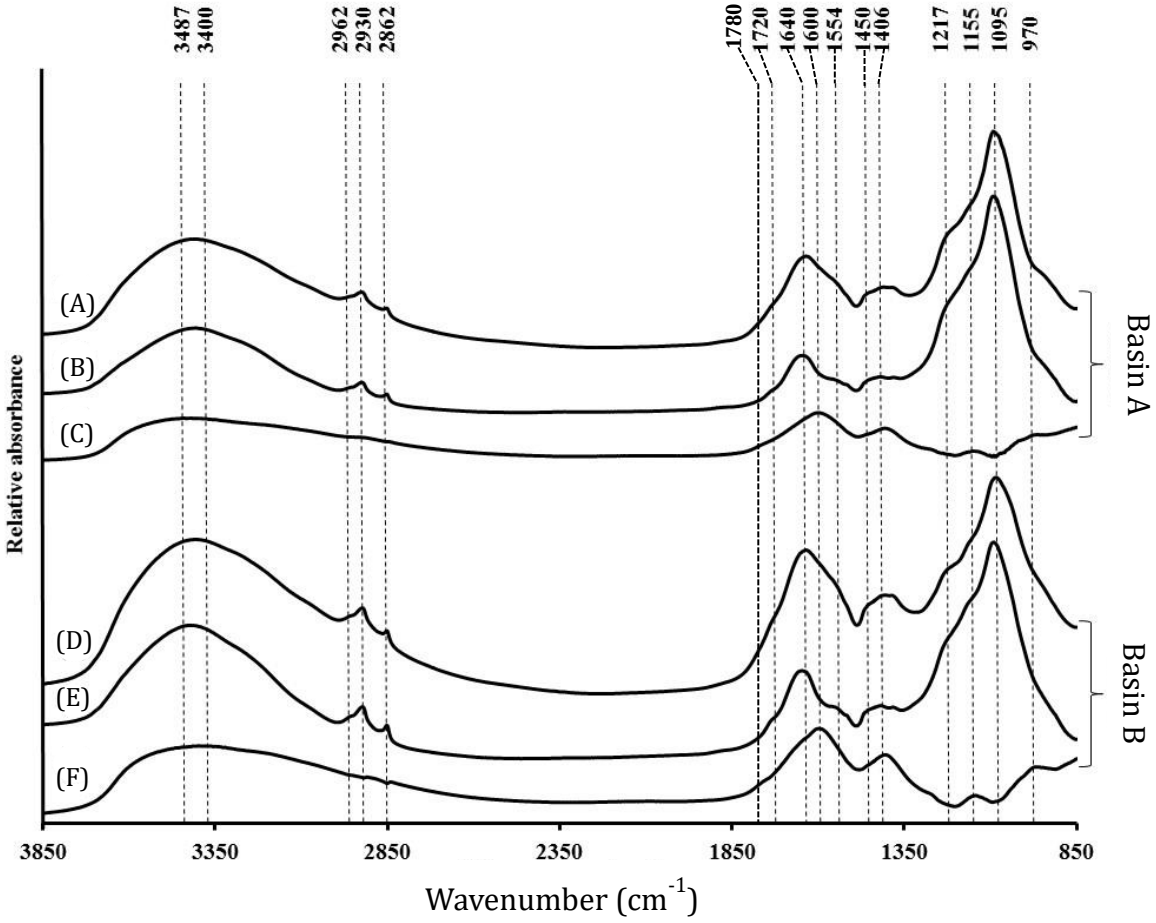

Figure 4. FTIR spectra of the initial (A and D), residual (B and E) and Fe-associated (C and F) OM for surface sediment (1-2 cm) of basin A (top) and basin B (bottom).

The largest peak in the spectra at 1095 cm^{-1}, caused by the antisymmetric motion of silicon atoms (υ_{as}-Si-O-Si) (Swann and Patwardhan, 2011) in Si-containing minerals (quartz and clays), was used as an internal standard to normalize the spectra since its abundance did not vary with depth in the sediments, and because Si-containing minerals are resistant to the dithionite treatment as it is seen when comparing spectra A and B for basin A and spectra D and E for basin B in Figure 4 (Kovač et al., 2006). Combined with the precise and constant sediment-to-KBr mass ratio used when preparing the pellets, normalizing the spectra in this way allowed estimating the composition of the Fe-associated OM fraction by difference (spectrum before the reduction treatment minus spectrum after the treatment = spectrum of Fe-associated OM). The resulting three spectra were compared to assess differences such as wavelength shifts, variation in intensity or appearance of new peaks, reflecting differences in OM composition and/or direct chemical environment. The relative intensities of the different peaks were not quantified owing to the uncertainty associated to the normalization, the spectra subtraction and the fact that several bands are not well resolved and appear as a shoulder on the neighboring band. Hence, the comparison below therefore must be considered semi-quantitative.

A series of absorbance bands were present in all samples: (1) a broad band between 3800 and 2600 cm^{-1}, centered around 3450 cm^{-1}, corresponding to the stretching band of hydrogen in the O-H groups of alcohols, phenols, or carboxylic acids, as well as to amide hydrogen stretching; (2) absorption bands representing C-H

stretching of methyl and aldehyde functional groups near 2962, 2930 and 2862 cm^{-1}; (3) a shoulder at 1780 cm^{-1} for C=O stretch of COOH, asymmetric COO^- stretch at 1600 to 1650 cm^{-1}, symmetric COO^- stretch at 1406 cm^{-1} (Chorover and Amistadi, 2001); (4) bands corresponding to aromatic structures in the 1500 to 1620 cm^{-1} range; (5) the wavenumber region between 1470 and 1380 cm^{-1} is attributed to CH_2 and CH_3 bending; (6) a large band between 1000 and 1155 cm^{-1} corresponding to the stretching of C-O group for the tertiary, secondary, and primary alcohols at about 1155, 1120, and 1070 cm^{-1} (Stevenson, 1994). Because of the presence of the intense silica band at 1095 cm^{-1}, the alcohol bands appear as shoulders on either side of the 1095 cm^{-1} band. The bands below 1000 cm^{-1} were not interpreted because of the potential presence of bands attributable to minerals.

The infrared spectra of total OM were similar at each depth in the two basins (Figure 4 and Figures S1-S3 in the Supporting Information section), with intensities relative to the silica band generally slightly lower at depth compared to the surface in both basins, as well as in Basin A compared to Basin B for equivalent depths (Figure S1). A similar pattern was observed for the Fe-associated (Figure S2) and the residual (Figure S3) OM. This result suggests that the contrasting bottom water redox conditions in the two basins did not lead to FTIR-visible differences in the speciation of sedimentary OM as the same functional groups with similar relative intensities were found in the different fractions of samples taken at equivalent depths. Also it is noteworthy that not only the composition of the Fe-associated OM fraction, residual and non Fe-associated OM fractions remained similar over more than 200 years, but also that they did not vary

much with depth in each core (Figures S2 and S3). As the sediments are depleted in oxygen in both basins (except at the surface of Basin A), this result agrees with the reported stability of Fe-OM aggregates in anoxic settings (Lalonde et al., 2012). It also means that OM composition likely is not the reason for the different Fe-OC ratios measured in the two basins, as opposed to the presence of an iron mineral with a lower affinity for OM than iron hydroxides, most likely iron sulfide. Note however that iron sulfide also plays an important role in the preservation of OM in sediments, as shown by recent published reports (Ma et al., 2022; Nabeh et al., 2022; Picard et al., 2019; Tétrault and Gélinas, 2022). Our results hence suggest that OM associated with FeS in our samples (not assessed here as no method currently exists to quantify FeS-associated OM) is compositionally similar to OM associated with Fe hydroxides.

There were however important differences when comparing the chemical composition of the three OM fractions for each sample. While the differences in spectral peak shapes and intensities for total OM and residual OM were small, the differences between these two fractions and Fe-associated OM were striking. First, there was a clear change in peak shape and a shift of the O-H/N-H band between 3850 and 2600 cm^{-1} towards higher wavenumbers, with a maximum peak intensity shifted from 3450 to 3525 cm^{-1} for Basin A. This shift is diagnostic for a higher relative intensity of the O-H functionality with respect to the N-H stretching band in Fe-associated OM and agrees with the lower C:N atomic ratios of Fe-associated OM compared to initial and residual OM (Figures 3A and 3D).

One of the most intriguing characteristic of Fe-associated OM is the almost complete absence on the C-H stretch (2960/2930/2860 cm^{-1}) and CH_2/CH_3 bending (1470/1380 cm^{-1}) bands (the latter two bands at 1470 and 1380 cm^{-1} appear as shoulders of the more intense 1410 cm^{-1} peak on the spectra of total and residual OM). These bands are present in most FTIR spectra of natural OM and point to highly aromatic or heteroatomic organic structures associated with iron oxides.

The carbonyl and aromatic bands also differ in the Fe-associated OM spectra. First, a small shoulder at 1780 cm^{-1} is more clearly defined, although this could simply be due to the generally lower spectral relative abundances for Fe-associated OM. More importantly, there was a clear shift of the maximum intensity for the carboxyl asymmetric stretch peak from 1640 cm^{-1} in the spectrum for total OM to 1600 cm^{-1} in the spectrum for Fe-associated OM (Gu et al., 1994). Although aromatic C=C functional groups also have a stretching absorption in the same region (1600 cm^{-1}), the existence of a strong absorption band at 1400 cm^{-1}, which is more pronounced in the spectrum for Fe-associated OM, is consistent with the formation of metal-carboxylate complexes, as shown in other studies (Biber and Stumm, 1994; Jones and Edwards, 1998; Guan et al., 2006; Eusterhues et al., 2010). Interestingly, a small peak centered at 1150 cm^{-1} is apparent in the spectra of Fe-associated OM. This peak corresponds to tertiary alcohols as would be found in lignin phenols, which are known for their high affinity for iron oxides (Niemeyer et al., 1992; Gu et al., 1994; Ilani et al., 2005).

These spectral differences between Fe-associated OM and total or residual OM correspond to the functional groups lost when reductively removing the iron oxides.

They provide clues on the type of compounds that readily associate with iron oxides in sediments and that remain part of the solid phase only because of their association with this mineral phase. These compounds are hydrophilic, aromatic- and carboxylic-rich, depleted in nitrogen, and with tertiary O-H groups, analogous to lignin and tannin degradation products.

The FTIR analyses also provide information on the type of chemical bonds between the organic moieties and iron oxides (Fu and Quan, 2006). In particular, the bands at 1600 and 1400 cm^{-1} (Figure 4c and 4f) support the relevance of inner-sphere interactions as an important mechanism of complexation of sedimentary OM with Fe oxides, in agreement with the conclusions of Lalonde et al. (2012) and Borowski et al (2018). These results also suggest that complexation is taking place independently of sediment redox conditions near the SWI, as long as a redox boundary exists where iron oxides can form in the presence of dissolved or particular OM (i.e., most likely in the water column, as in Basin B, or in the sediment/at the SWI as in Basin A). Complexation and adsorption of OM on the surface of iron oxides, or coprecipitation with iron oxides, are thus complementary mechanisms of association between Fe oxides and OM, whose relative importance depends on local conditions (mostly oxidation-reduction potential, but also the abundance of iron, OM and competing ligands such as sulfides). More work is needed to fully understand the fine controls on these competing reactions in sedimentary environments. Noteworthy, the similar chemical composition of Fe-associated OM in both basins and at different depths suggests that the large differences in OC:Fe and TN:Fe ratios measured between the two basins most likely were not linked

to differences in OM abundance, composition or reactivity, but rather to differences linked to Fe cycling in the two basins, and in particular to the higher abundance of AVS in Basin B (Couture et al., 2007; 2008). Mackinawite (FeS), a form of AVS resulting from the reaction of dissolved Fe(II) and sulfides in the pore water, is unstable under oxic conditions. Its oxidation to iron oxides during freeze-drying likely contributed to the higher reactive iron pool in Basin B, artificially decreasing the measured OC:Fe given that mackinawite, which formed by Fe(II) and HS^- under anoxic conditions, has a lower affinity towards natural OM compared to iron hydroxides, while still playing an important but yet-to-be quantified role in natural sedimentary OM preservation (Ma et al., 2022; Nabeh et al., 2022; Picard et al., 2019; Tétrault and Gélinas, 2022).

There are several implications to our results. First, the OC preservation mechanism reported by Lalonde et al. (2012) for marine sediments also plays an important role in lacustrine sediments, as shown in Lake Tantaré where about 30% of the total OC is closely associated with iron hydroxides. Second, the absolute redox potential is not the main factor explaining the formation of Fe-OM aggregates. The redox boundary where Fe(II) is oxidized to Fe(III) and precipitated as amorphous iron hydroxide phases in the presence of dissolved OC most likely is key. These aggregates appear stable on long timescales under anoxic conditions likely because the Fe oxides are poisoned by co-precipitated OM, making them less readily available to iron-reducing bacteria. However, they are probably degraded when exposed to oxidizing conditions on long time scales through non-specific OM oxidation reactions involving activated oxygen species. This Fe-OM complexation mechanism thus acts as a shuttle that actively

transfers reactive OM from oxic to anoxic settings while partially protecting it from enzymatic and chemolytic attack. Third, the formation of Fe-OM aggregates likely is driven by OM composition, as there were no compositional differences in Fe-associated OM between cores or sediment depths. Fourth, mackinawite and other iron sulfide species may contribute to the measured reactive Fe pool and may therefore artificially decrease the OC:Fe ratios acquired using this method. Care must thus be taken when using OC:Fe ratios as a diagnostic tool in reducing sediments to apportion inner- *vs.* outer-sphere reactions, as done by Lalonde et al. (2012). Moreover, OC:Fe ratios when accumulating under oxic conditions, could be misleading as the proportion of reactive iron oxides associated with OM varies from sample to sample and reaches a maximum only in sulfidic sediments (Barber et al., 2014).

More work is needed to untangle the complex web of reactions involving OM and Fe in sediments, including the kinetics of the competing reactions and the interaction between organic matter and iron-sulfide minerals, especially mackinawite (FeS). Importantly, studies such as this one, which focuses on the chemistry of Fe-OM interactions, should be paralleled by others assessing the role of bacteria in the direct and indirect formation and degradation of Fe-OM complexes.

Acknowledgments

This research was made possible thanks to financial support provided by Natural Science and Engineering Research Council of Canada (Grant Number RGPIN-2018-

05080), the Canadian Foundation for Innovation (Grant Number 7548), as well as Concordia University.

Author contributions

All authors contributed to the study conception and design. Material preparation, data collection and analysis were performed by Azadeh Joshani and Andrew Barber. The manuscript was written by Azadeh Joshani, Yeganeh Mirzaei and Yves Gélinas. Yeganeh Mirzaei reviewed the results and helped with the interpretations, edited the text, modified Figure 4, designed Figures 2 and 3, as well as the graphical abstract of this paper. All authors commented on previous versions of the manuscript and approved the final manuscript.

Data availability

The datasets generated during the current study are available in the Supporting Information section.

Literature cited

Alfaro-De la Torre, M.C., Beaulieu, P.-Y. and Tessier, A., 2000. In situ measurement of trace metals in lakewater using the dialysis and DGT techniques. *Analytica Chimica Acta* **418**, 53-68.

Arnarson, T.S. and Keil, R.G., 2007. Changes in organic matter–mineral interactions for marine sediments with varying oxygen exposure times. *Geochimica et Cosmochimica Acta* **71**, 3545-3556.

Barber, A., Brandes, J., Leri, A, Lalonde, K., Balind, K., Wirick, S., Wang, J., Gélinas, Y., 2017. Preservation of organic matter in marine sediments by inner-sphere interactions with reactive iron. *Scientific Reports* **7**: 366. DOI:10.1038/s41598-017-00494-0.

Barber, A., Lalonde, K., Mucci, A. and Gélinas, Y., 2014. The role of iron in the diagenesis of organic carbon and nitrogen in sediments: A long-term incubation experiment. *Marine Chemistry* **162**, 1-9.

Berner, R.A., 1970. Sedimentary pyrite formation. *American Journal of Science* **268**, 1-23.

Betts, J. and Holland, H., 1991. The oxygen content of ocean bottom waters, the burial efficiency of organic carbon, and the regulation of atmospheric oxygen. *Palaeogeography, Palaeoclimatology, Palaeoecology* **97**, 5-18.

Biber, M.V. and Stumm, W., 1994. An in-situ ATR-FTIR study: The surface coordination of salicylic acid on aluminum and iron (III) oxides. *Environmental Science and Technology* **28**, 763-768.

Bordovskiy, O., 1965. Transformation of organic matter in bottom sediments and its early diagenesis. *Marine Geology* **3**, 83-114.

Borowski, S.C., Biswakarma, J., Kang, K., Schenkeveld, W.D.C., Hering, J.G., Kubicki, J.D., Kraemer, S.M., Hug, S.J., 2018. Structure and reactivity of oxalate surface complexes on lepidocrocite derived from infrared spectroscopy, DFT-calculations,

adsorption, dissolution and photochemical experiments. *Geochimica et Cosmochimica Acta* **226**, 244-262.

Botrel, M., Gregory-Eaves, I. and Maranger, R., 2014. Defining drivers of nitrogen stable isotopes ($\delta^{15}N$) of surface sediments in temperate lakes. *Journal of Paleolimnology* **52**, 419-433.

Boudot, J., Hadj, A.B., Steiman, R. and Seigle-Murandi, F., 1989. Biodegradation of synthetic organo-metallic complexes of iron and aluminium with selected metal to carbon ratios. *Soil Biology and Biochemistry* **21**, 961-966.

Burdige, D.J., 2007. Preservation of organic matter in marine sediments: controls, mechanisms, and an imbalance in sediment organic carbon budgets? *Chemical Reviews* **107**, 467-485.

Canfield, D.E., 1994. Factors influencing organic carbon preservation in marine sediments. *Chemical Geology* **114**, 315-329.

Chappaz, A., Gobeil, C. and Tessier, A., 2008. Geochemical and anthropogenic enrichments of Mo in sediments from perennially oxic and seasonally anoxic lakes in Eastern Canada. *Geochimica et Cosmochimica Acta* **72**, 170-184.

Chorover, J. and Amistadi, M.K., 2001. Reaction of forest floor organic matter at goethite, birnessite and smectite surfaces. *Geochimica et Cosmochimica Acta* **65**, 95-109.

Clow, D. W. *et al.*, 2015. Organic Carbon Burial in Lakes and Reservoirs of the Conterminous United States. *Environmental Science and Technology* **49**, 7614–7622.

Cole, J.J., Cole, J.J., Caraco, N.F. and Caraco, N.F., 2001. Carbon in catchments: connecting terrestrial carbon losses with aquatic metabolism. *Marine and Freshwater Research* **52**, 101-110.

Couture, R.-M., Gobeil, C. and Tessier, A., 2008. Chronology of atmospheric deposition of arsenic inferred from reconstructed sedimentary records. *Environmental Science and Technology* **42**, 6508-6513.

Couture, R.-M., Shafei, B., Van Cappellen, P., Tessier, A. and Gobeil, C., 2009. Non-steady state modeling of arsenic diagenesis in lake sediments. *Environmental Science and Technology* **44**, 197-203.

Couture, R.-M., Fischer, R., Van Cappellen, P., Gobeil, C., 2016. Non-steady state diagenesis of organic and inorganic sulfur in lake sediments. *Geochimica et Cosmochimica Acta* **194**, 15-33.

Coward E.K., Ohno, T., Sparks, D.L., 2018. Direct evidence for temporal molecular fractionation of dissolved organic matter at the iron oxyhydroxide interface. Environmental Science and Technology. DOI: 10.1021/acs.est.8b04687.

Demaison, G. and Moore, G.T., 1980. Anoxic environments and oil source bed genesis. *AAPG Bulletin* **64**, 1179-1209.

Eusterhues, K., Rennert, T., Knicker, H., Kögel-Knabner, I., Totsche, K.U., and Schwertmann, U., 2010. Fractionation of organic matter due to reaction with ferrihydrite: coprecipitation versus adsorption. *Environmental Science and Technology* **45**, 527-533.

Falkowski, P. *et al.*, 2000. The global carbon cycle: a test of our knowledge of earth as a system. *Science* **290**, 291-296.

Ferland, M.E., Giorgio, P.A., Teodoru, C.R. and Prairie, Y.T., 2012. Long-term C accumulation and total C stocks in boreal lakes in northern Québec. *Global Biogeochemical Cycles* **26**, GB0E04.

Feyte, S., Tessier, A., Gobeil, C. and Cossa, D., 2010. In situ adsorption of mercury, methylmercury and other elements by iron oxyhydroxides and organic matter in lake sediments. *Applied Geochemistry* **25**, 984-995.

Feyte, S., Gobeil, C., Tessier, A. and Cossa, D., 2012. Mercury dynamics in lake sediments. *Geochimica et Cosmochimica Acta* **82**, 92-112.

Fortin, D., Leppard, G.G. and Tessier, A., 1993. Characteristics of lacustrine diagenetic iron oxyhydroxides. *Geochimica et Cosmochimica Acta* **57**, 4391-4404.

Fu, H. and Quan, X., 2006. Complexes of fulvic acid on the surface of hematite, goethite, and akaganeite: FTIR observation. *Chemosphere* **63**, 403-410.

Galy, V. *et al.*, 2007. Efficient organic carbon burial in the Bengal fan sustained by the Himalayan erosional system. *Nature* **450**, 407-410.

Gu, B., Schmitt, J., Chen, Z., Liang, L. and McCarthy, J.F., 1994. Adsorption and desorption of natural organic matter on iron oxide: mechanisms and models. *Environmental Science and Technology* **28**, 38-46.

Guan, X.-H., Shang, C. and Chen, G.-H., 2006. ATR-FTIR investigation of the role of phenolic groups in the interaction of some NOM model compounds with aluminum hydroxide. *Chemosphere* **65**, 2074-2081.

Haese, R.R., Wallmann, K., Dahmke, A., Kretzmann, U., Müller, P.J. and Schulz, H.D., 1997. Iron species determination to investigate early diagenetic reactivity in marine sediments. *Geochimica et Cosmochimica Acta* **61**, 63–72.

Hamilton-Taylor, J., Willis, M. and Reynolds, C., 1984. Depositional fluxes of metals and phytoplankton in Windermere as measured by sediment traps. *Limnology and Oceanography* **29**, 695-710.

Hartnett, H.E., Keil, R.G., Hedges, J.I. and Devol, A.H., 1998. Influence of oxygen exposure time on organic carbon preservation in continental margin sediments. *Nature* **391**, 572-575.

Hartnett, H.E. and Devol, A.H., 2003. Role of a strong oxygen-deficient zone in the preservation and degradation of organic matter: A carbon budget for the continental margins of northwest Mexico and Washington State. *Geochimica et Cosmochimica Acta* **67**, 247-264.

Hedges, J.I. and Stern, J.H., 1984. Carbon and Nitrogen Determinations of Carbonate-Containing Solids. Limnology and Oceanography, 29, 657-663.

Hedges, J.I. and Keil, R.G., 1995. Sedimentary organic matter preservation: an assessment and speculative synthesis. *Marine Chemistry* **49**, 81-115.

Heiri, O., Lotter, A.F. and Lemcke, G., 2001. Loss on ignition as a method for estimating organic and carbonate content in sediments: reproducibility and comparability of results. *Journal of Paleolimnology* **25**, 101-110.

Henrichs, S.M. and Reeburgh, W.S., 1987. Anaerobic mineralization of marine sediment organic matter: rates and the role of anaerobic processes in the oceanic carbon economy. *Geomicrobiology Journal* **5**, 191-237.

Ilani, T., Schulz, E. and Chefetz, B., 2005. Interactions of organic compounds with wastewater dissolved organic matter. *Journal of Environmental Quality* **34**, 552-562.

Ingalls, A.E., Lee, C., Wakeham, S.G. and Hedges, J.I., 2003. The role of biominerals in the sinking flux and preservation of amino acids in the Southern Ocean along 170°W. *Deep Sea Research Part II: Topical Studies in Oceanography* **50**, 713-738.

Jones, D. and Edwards, A., 1998. Influence of sorption on the biological utilization of two simple carbon substrates. *Soil Biology and Biochemistry* **30**, 1895-1902.

Kaiser, K., Guggenberger, G., Haumaier, L. and Zech, W., 1997. Dissolved organic matter sorption on sub soils and minerals studied by ^{13}C-NMR and DRIFT spectroscopy. *European Journal of Soil Science* **48**, 301-310.

Keil, R.G., Montluçon, D.B. and Prahl, F.G., 1994. Sorptive preservation of labile organic matter in marine sediments. *Nature* **370**, 18.

Kennedy, M.J. and Wagner, T., 2011. Clay mineral continental amplifier for marine carbon sequestration in a greenhouse ocean. *Proceedings of the National Academy of Sciences* **108**, 9776-9781.

Kovač, N. *et al.*, 2006. Degradation and preservation of organic matter in marine macroaggregates. *Acta Chimica Slovenia* **53**, 81-87.

Laforte, L., Tessier, A., Gobeil, C. and Carignan, R., 2005. Thallium diagenesis in lacustrine sediments. *Geochimica et Cosmochimica Acta* **69**, 5295-5306.

Lalonde, K., Mucci, A., Ouellet, A. and Gélinas, Y., 2012. Preservation of organic matter in sediments promoted by iron. *Nature* **483**, 198-200.

Liu, K., Wu, L., Couture, R.-M., Li, W. and Van Cappellen, P., 2015. Iron isotope fractionation in sediments of an oligotrophic freshwater lake. *Earth and Planetary Science Letters* **423**, 164-172.

Ma, W.-W., Zhu, M.-X., Yang, G.-P., Li, T., Li, Q.-Q., Liu, S.-H. and Li, J.-L., 2022. Stability and molecular fractionation of ferrihydrite-bound organic carbon during iron reduction by dissolved sulfide. Chemical Geology **594**, 120774.

Mackey, D.J., Zirino, A., 1994. Comments on trace metal speciation in seawater or do "onions" grow in the sea? *Analytica Chimica Acta* **284 (3)**, 635-647.

Mayer, L.M., 1995. Sedimentary organic matter preservation: an assessment and speculative synthesis—a comment. *Marine Chemistry* **49**, 123-126.

Mehra, O.P. and Jackson, M.L., 1960. Iron oxide removal from soils and clays by a dithionite-citrate system buffered with sodium bicarbonate. *Clays and Clay minerals* **7**, 317-327.

Müller, P.J. and Suess, E., 1979. Productivity, sedimentation rate, and sedimentary organic matter in the oceans—I. Organic carbon preservation. *Deep Sea Research Part A. Oceanographic Research Papers* **26**, 1347-1362.

Nabeh, N., Brokaw, C., Picard, A., 2022. Quantification of organic carbon sequestered by biogenic iron sulfide minerals in long-term anoxic laboratory incubations. *Frontiers in Microbiology*. doi: 10.3389/fmicb.2022.662219.

Niemeyer, J., Chen, Y. and Bollag, J.-M., 1992. Characterization of humic acids, composts, and peat by diffuse reflectance Fourier-transform infrared spectroscopy. *Soil Science Society of America Journal* **56**, 135-140.

Pace, M.L. and Prairie, Y.T., 2005. Respiration in lakes. *Respiration in aquatic ecosystems*, 103-121.

Paropkari, A.L., Babu, C.P. and Mascarenhas, A.A., 1992. critical evaluation of depositional parameters controlling the variability of organic carbon in Arabian Sea sediments. *Marine Geology* **107**, 213-226.

Picard, A., Gartman, A., Cosmidis, J., Obst, M., Vidoudez, C., Clarke, D.R. and Girguis, P.R., 2019. Authigenic metastable iron sulfide minerals preserve microbial organic carbon in anoxic environments. *Chemical Geology* **530**, 119343.

Sobek, S., Algesten, G., Bergström, A. K., Jansson, M. and Tranvik, L.J., 2003. The catchment and climate regulation of pCO_2 in boreal lakes. *Global Change Biology* **9**, 630-641.

Stevenson, F.J., 2004. *Humus Chemistry: Genesis, Composition, Reactions*. In: John Wiley and Sons.

Straub, K.L., Benz, M., Schink, B. and Widdel, F., 1996. Anaerobic, nitrate-dependent microbial oxidation of ferrous iron. *Applied and Environmental Microbiology* **62**, 1458-1460.

Swann, G.E. and Patwardhan, S., 2011. Application of Fourier Transform Infrared Spectroscopy (FTIR) for assessing biogenic silica sample purity in geochemical analyses and palaeoenvironmental research. *Climate of the Past* **7**, 65-74.

Tessier, A., Gobeil, C. and Laforte, L., 2014. Reaction rates, depositional history and sources of indium in sediments from Appalachian and Canadian Shield lakes. *Geochimica et Cosmochimica Acta* **137**, 48–63. The electronic annex: http://dx.doi.org/10.1016/ j.gca.2014.03.042.

Tétrault, A., and Gélinas, Y., 2022. Preferential sorption of polysaccharides on mackinawite: A chemometrics approach. *Geochimica et Cosmochimica Acta* **337**, 61–72.

Thamdrup, B., Fossing, H. and Jørgensen, B.B., 1994. Manganese, iron and sulfur cycling in a coastal marine sediment, Aarhus Bay, Denmark. *Geochimica et Cosmochimica Acta* **58**, 5115-5129.

Thornton, S. and McManus, J., 1994. Application of organic carbon and nitrogen stable isotope and C/N ratios as source indicators of organic matter provenance in estuarine systems: evidence from the Tay Estuary, Scotland. *Estuarine, Coastal and Shelf Science* **38**, 219-233.

Viollier, E., Inglett, P., Hunter, K., Roychoudhury, A. and Van Cappellen, P., 2000. The ferrozine method revisited: Fe(II)/Fe(III) determination in natural waters. *Applied Geochemistry* **15**, 785-790.

Vitousek, P.M., Mooney, H.A., Lubchenco, J. and Melillo, J.M., 1997. Human domination of Earth's ecosystems. *Science* **277**, 494-499.

Wolthers, M., Charlet, L., Van der Linde, P.R., Rickard, D. and Van der Weijden, C.H., 2005. Surface chemistry of disordered mackinawite (FeS). Geochimica et Cosmochimica Acta, Vol. 69, No. 14, pp. 3469–3481.

Declaration of interests

☒ The authors declare that they have no known competing financial interests or personal relationships that could have appeared to influence the work reported in this paper.

☐ The authors declare the following financial interests/personal relationships which may be considered as potential competing interests:

Graphical Abstract

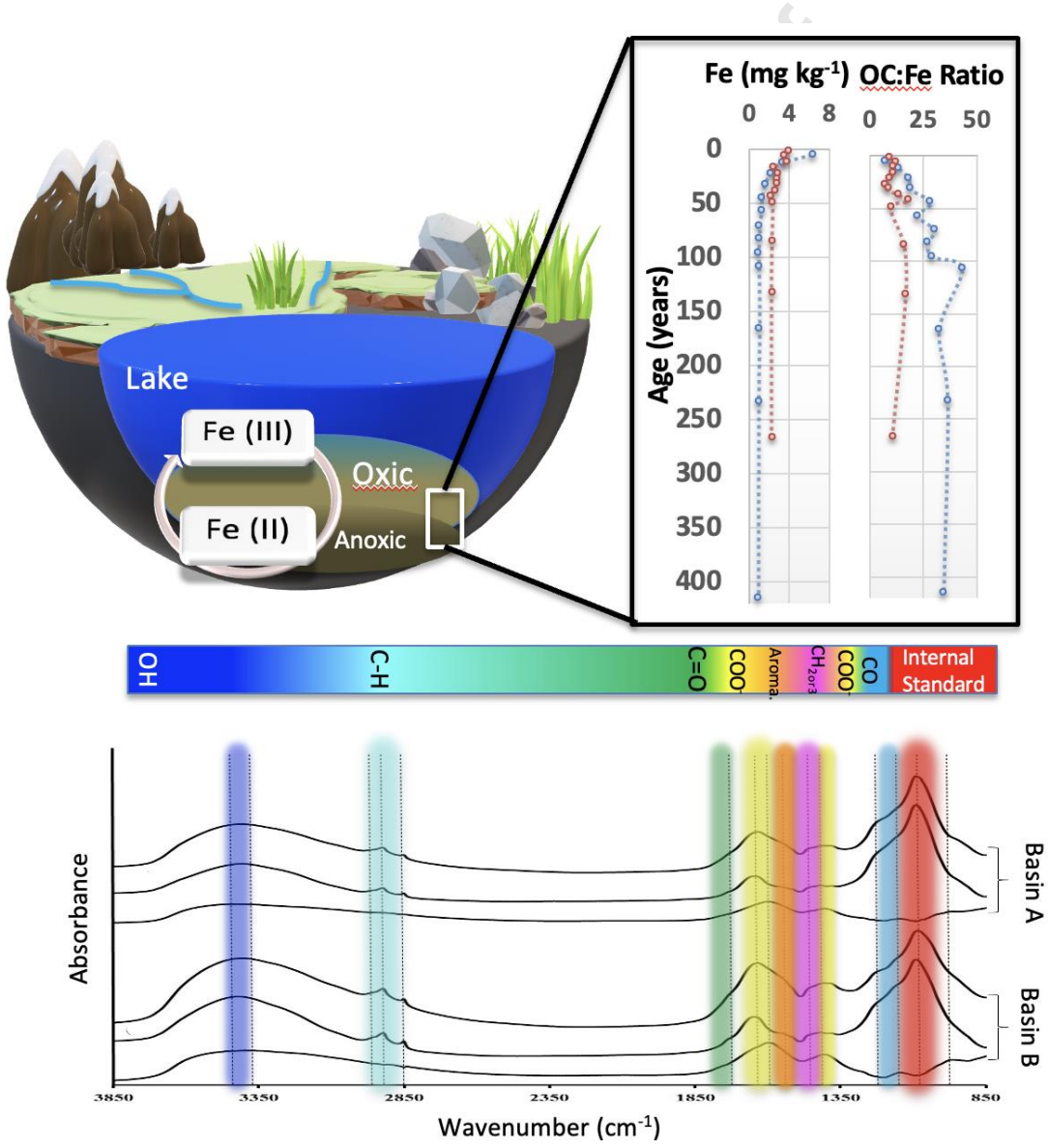

Highlights:

- Iron plays an important role in the preservation of lacustrine sedimentary organic matter
-
- Chemical composition of organic matter rather than redox conditions control the association between iron and organic matter
-
- OC:Fe ratios should not be used to infer a formation mechanism between iron and organic carbon